

## Supporting information for:

# Isolation of chloride- and hydride-bridged tri-iron and -zinc clusters in a tris( $\beta$ -oxo- $\delta$ -diimine) cyclophane ligand

Dae Ho Hong<sup>a</sup>, Brian Knight<sup>a</sup>, Vincent J. Catalano<sup>b</sup> and Leslie J. Murray\*<sup>a</sup>

<sup>a</sup>Department of Chemistry, Center for Catalysis, University of Florida, Gainesville, Florida 32611, United States

<sup>b</sup>Department of Chemistry, University of Nevada, Reno, Nevada 89557, United States

## Table of Contents

1. Physical Measurements.....	3
2. References .....	14

## Table of Figures

Figure S1. $^1\text{H}$ NMR spectrum ( $\text{CDCl}_3$ , 300 MHz) of $\text{H}_6\text{L}$ .....	3
Figure S2. Infrared spectrum of $\text{H}_6\text{L}$ .....	3
Figure S3. $^1\text{H}$ NMR spectrum ( $\text{C}_6\text{D}_6$ , 300 MHz) of $\text{H}_6\text{L}+3\text{LDA}$ .....	4
Figure S4. Infrared spectrum of $\text{H}_6\text{L}+3\text{LDA}$ .....	4
Figure S5. $^1\text{H}$ NMR spectrum ( $\text{C}_6\text{D}_6$ , 300 MHz) of $\text{H}_6\text{L}+6\text{LDA}$ .....	5
Figure S6. Infrared spectrum of $\text{H}_6\text{L}+6\text{LDA}$ .....	5
Figure S7. Paramagnetic $^1\text{H}$ NMR spectrum ( $\text{CDCl}_3$ , 500 MHz) of <b>1</b> .....	6
Figure S8. Infrared spectrum of <b>1</b> .....	6
Figure S9. $^1\text{H}$ NMR spectrum ( $\text{CDCl}_3$ , 500 MHz) of <b>2</b> .....	7
Figure S10. Infrared spectrum of <b>2</b> .....	7
Figure S11. Fe–Fe bond length plotted versus $\sin(\theta/2)$ , where $\theta$ is the angle of Fe–Cl–Fe. The slope represents twice the bond length of Fe–( $\mu$ -Cl). .....	8
Figure S12. Paramagnetic $^1\text{H}$ NMR spectrum ( $\text{C}_6\text{D}_6$ , 500 MHz) of <b>3</b> .....	9
Figure S13. Infrared spectrum of <b>3</b> .....	9
Figure S14. $^1\text{H}$ NMR spectrum ( $\text{C}_6\text{D}_6$ , 500 MHz) of <b>4</b> .....	10
Figure S15. Infrared spectrum of <b>4</b> .....	10
Figure S16. Cyclic voltammograms of <b>1</b> (0.87 mM) in THF using 0.30 M $[\text{Bu}_4\text{N}]^+\text{PF}_6^-$ as a supporting electrolyte. Ferrocene (1.1mM) was used as internal standard. Electrodes printed on a chip was used. Working electrode: Pt; reference electrode: Ag/AgCl; counter electrode: Pt; scan rate: 100–500 mV/s. ....	11
Figure S17. Cyclic voltammograms of <b>3</b> (0.87 mM) in THF using 0.30 M $[\text{Bu}_4\text{N}]^+\text{PF}_6^-$ as a supporting electrolyte. Ferrocene (1.1mM) was used as internal standard. Electrodes printed on a chip was	

used. Working electrode: Pt; reference electrode: Ag/AgCl; counter electrode: Pt; scan rate: 100–500 mV/s.....	11
Figure S18. $^1\text{H}$ NMR spectrum ( $\text{C}_6\text{D}_6$ , 500 MHz) of <b>3</b> + $\text{H}_2\text{O}$ .....	12
Figure S19. Infrared spectrum of <b>3</b> + $\text{H}_2\text{O}$ .....	12
Table 1. Crystal data and structure refinement for <b>1</b> .....	13

## 1. Physical Measurements

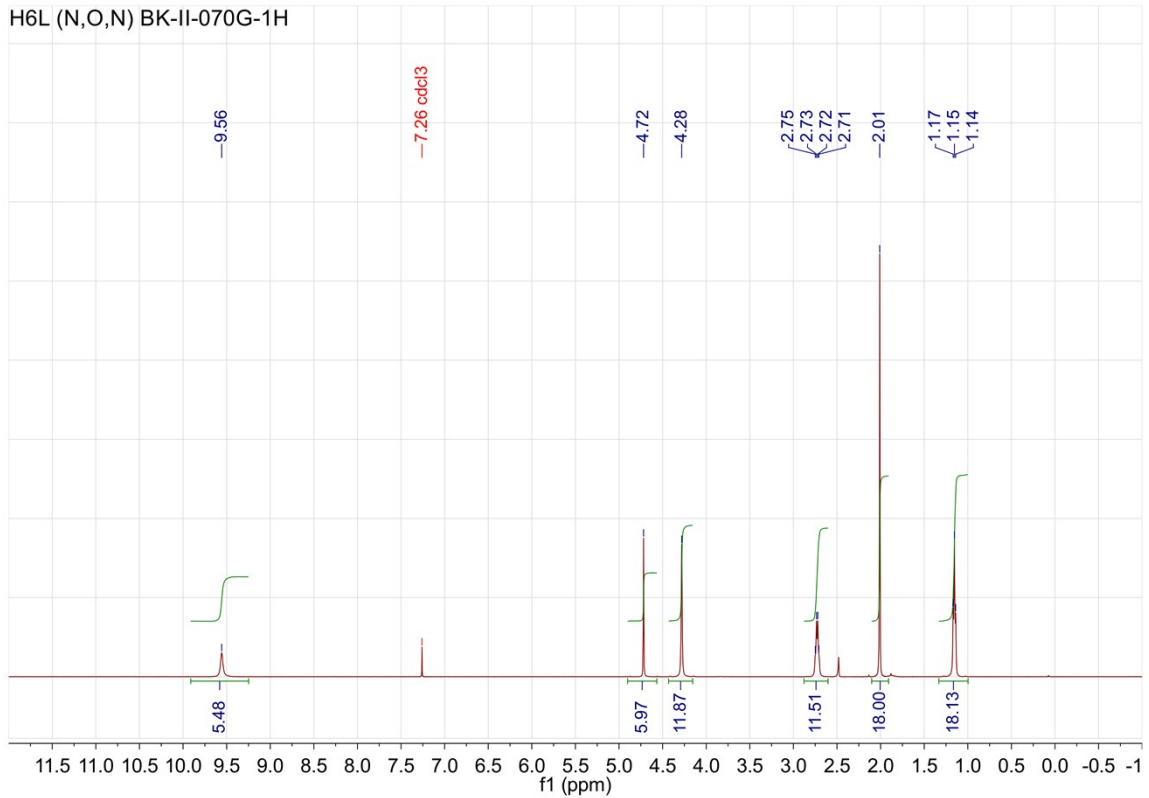


**Figure S1.**  $^1\text{H}$  NMR spectrum ( $\text{CDCl}_3$ , 300 MHz) of  $\text{H}_6\text{L}$

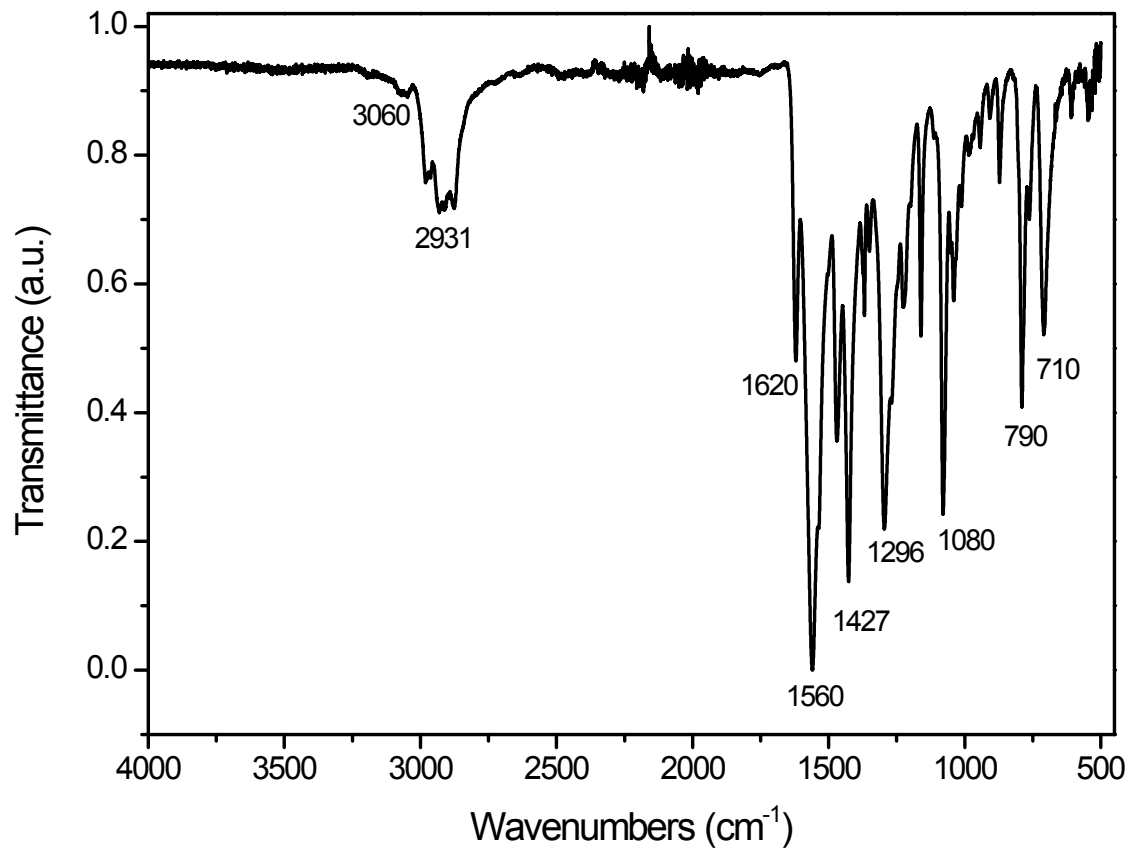


**Figure S2.** Infrared spectrum of  $\text{H}_6\text{L}$

DH-I-28\_3\_H6L\_NON\_3LDA\_in\_benzene

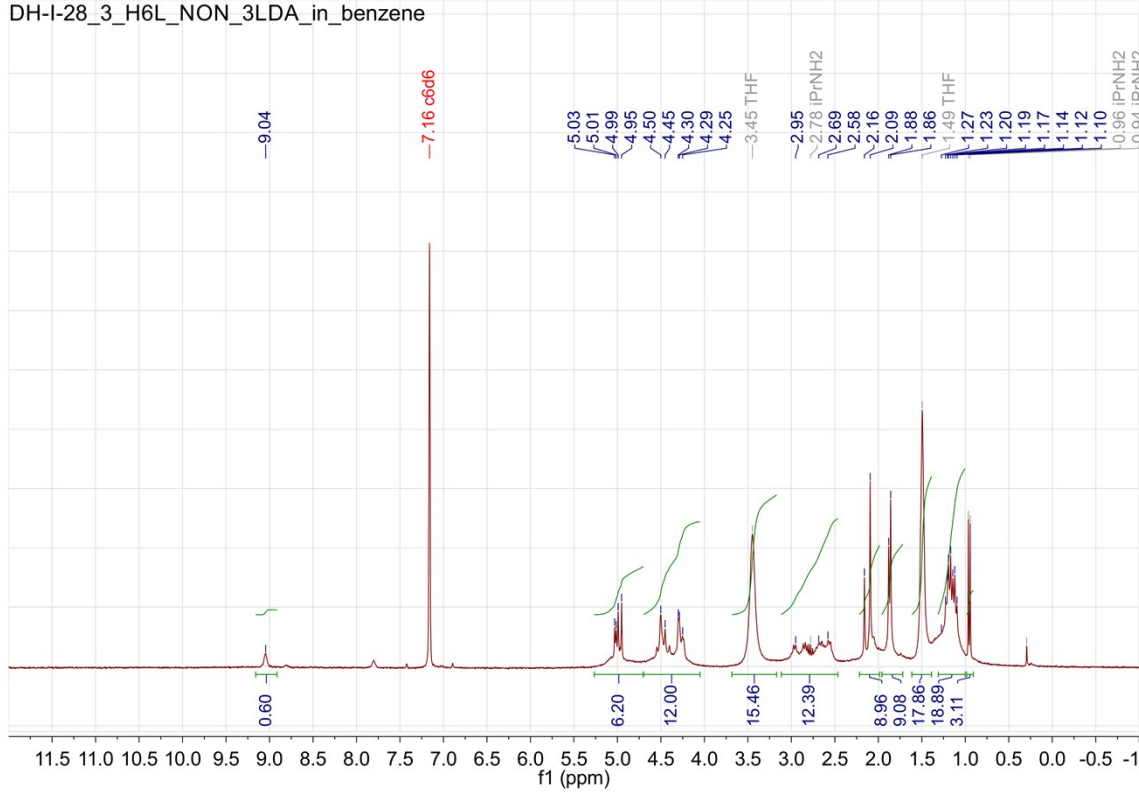


**Figure S3.** <sup>1</sup>H NMR spectrum ( $C_6D_6$ , 300 MHz) of  $H_6L+3LDA$

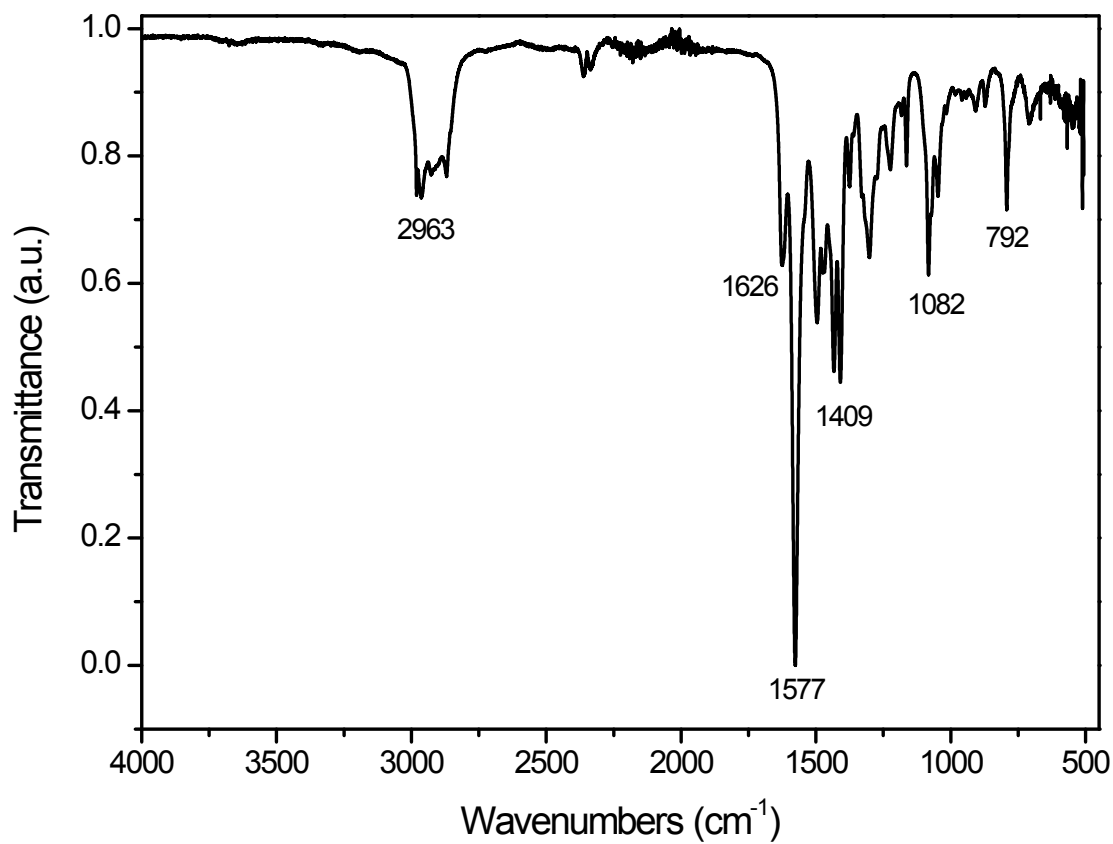


**Figure S4.** Infrared spectrum of  $H_6L+3LDA$

DH-I-28\_4\_H6L\_NON\_6LDA\_in\_benzene

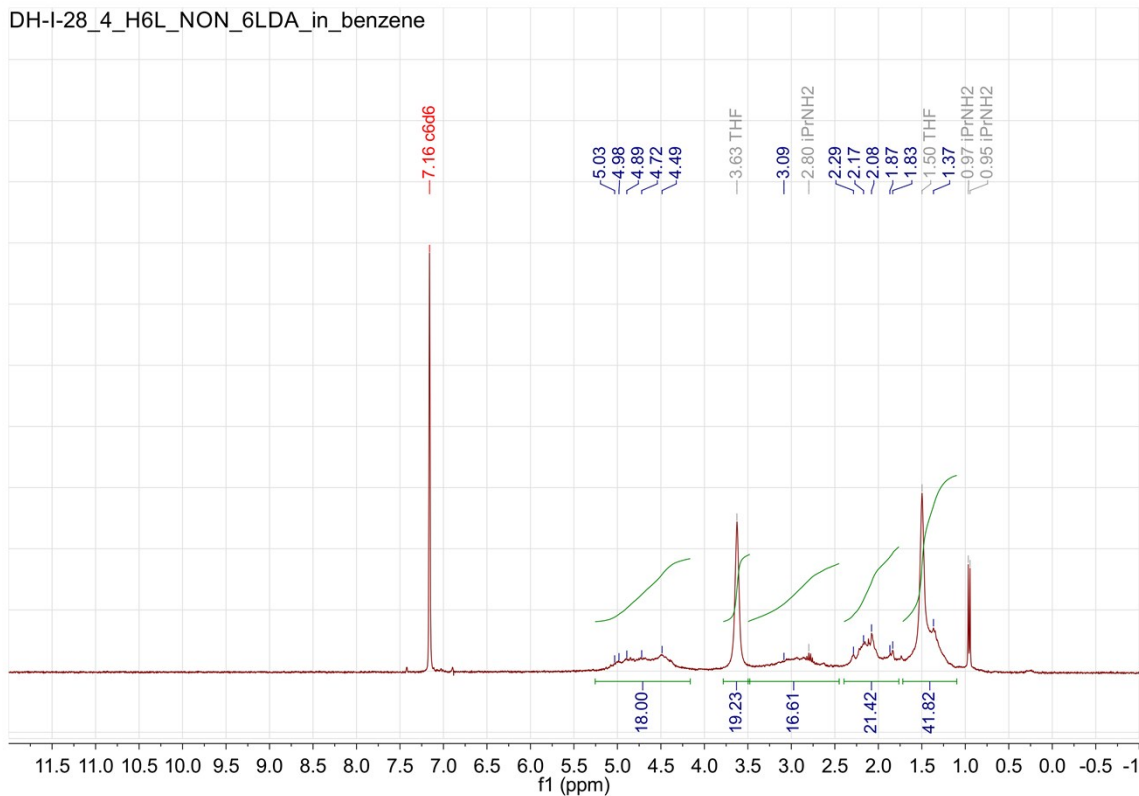


**Figure S5.** <sup>1</sup>H NMR spectrum ( $C_6D_6$ , 300 MHz) of  $H_6L+6LDA$

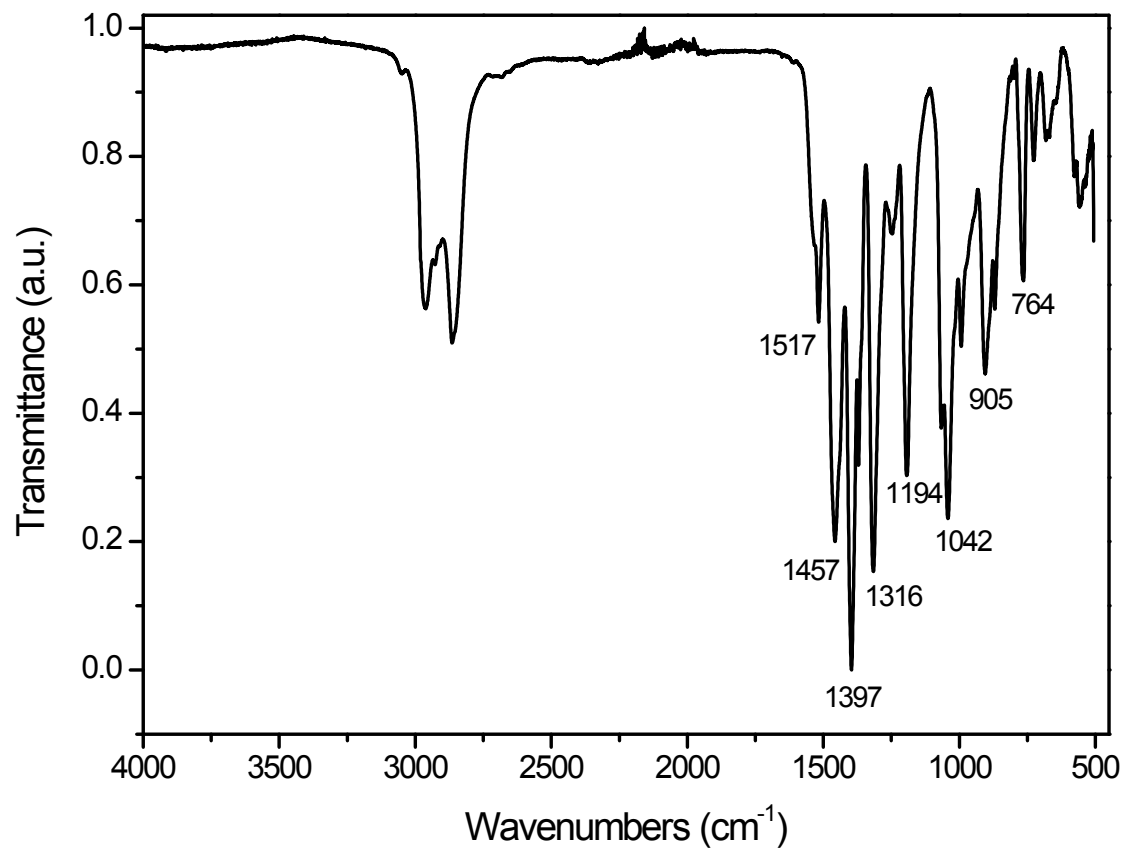


**Figure S6.** Infrared spectrum of  $H_6L+6LDA$

DH-I-104-1\_H3Fe3Cl3L\_NON\_PhCl\_CDCl<sub>3</sub>\_recry

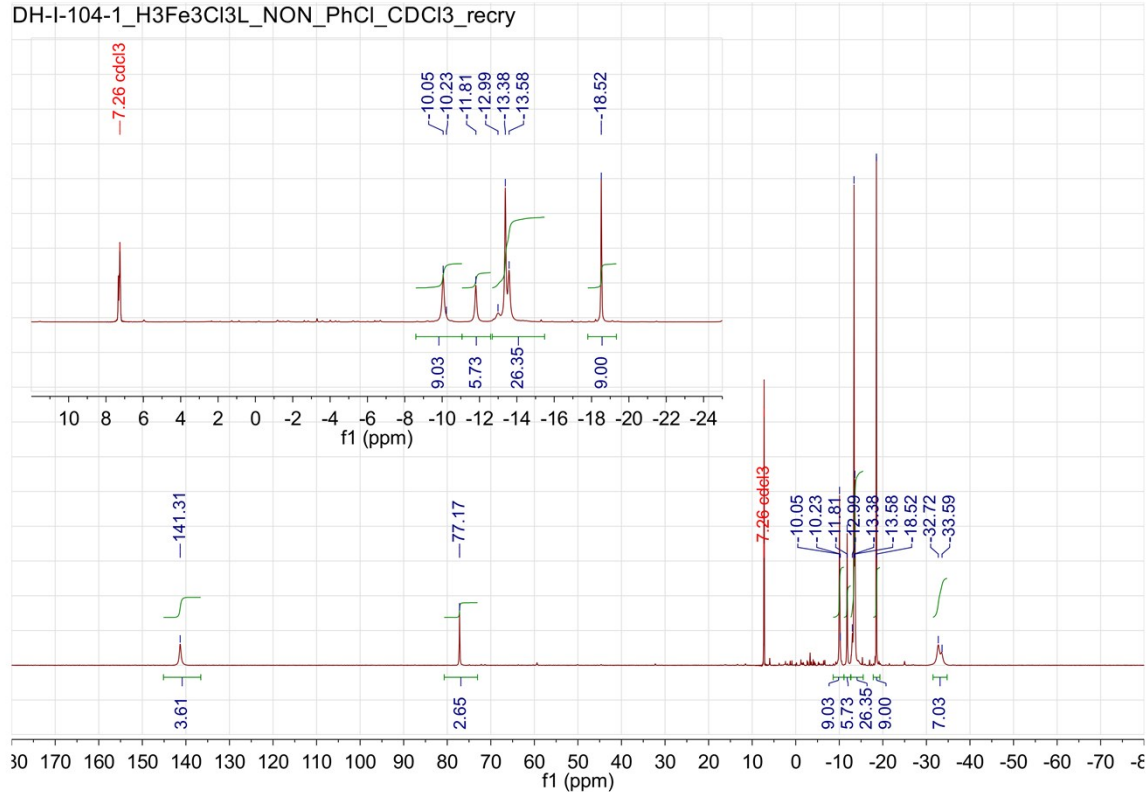


Figure S7. Paramagnetic <sup>1</sup>H NMR spectrum (CDCl<sub>3</sub>, 500 MHz) of **1**

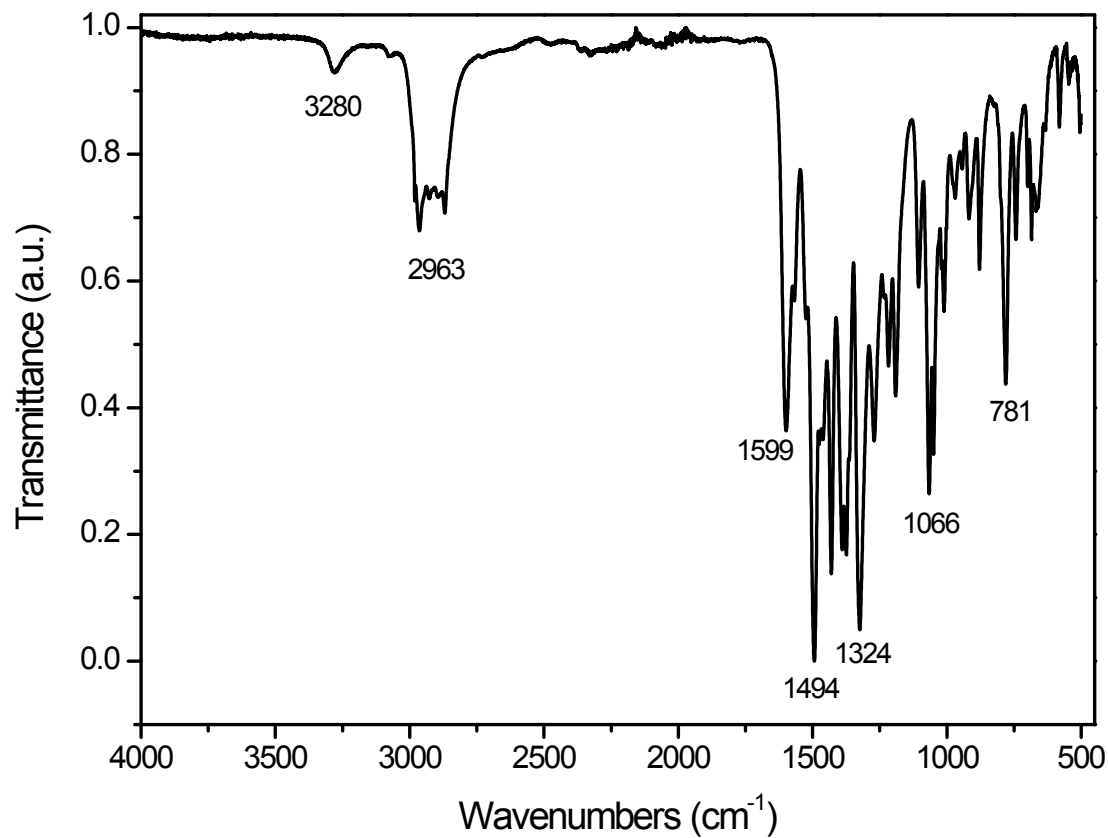
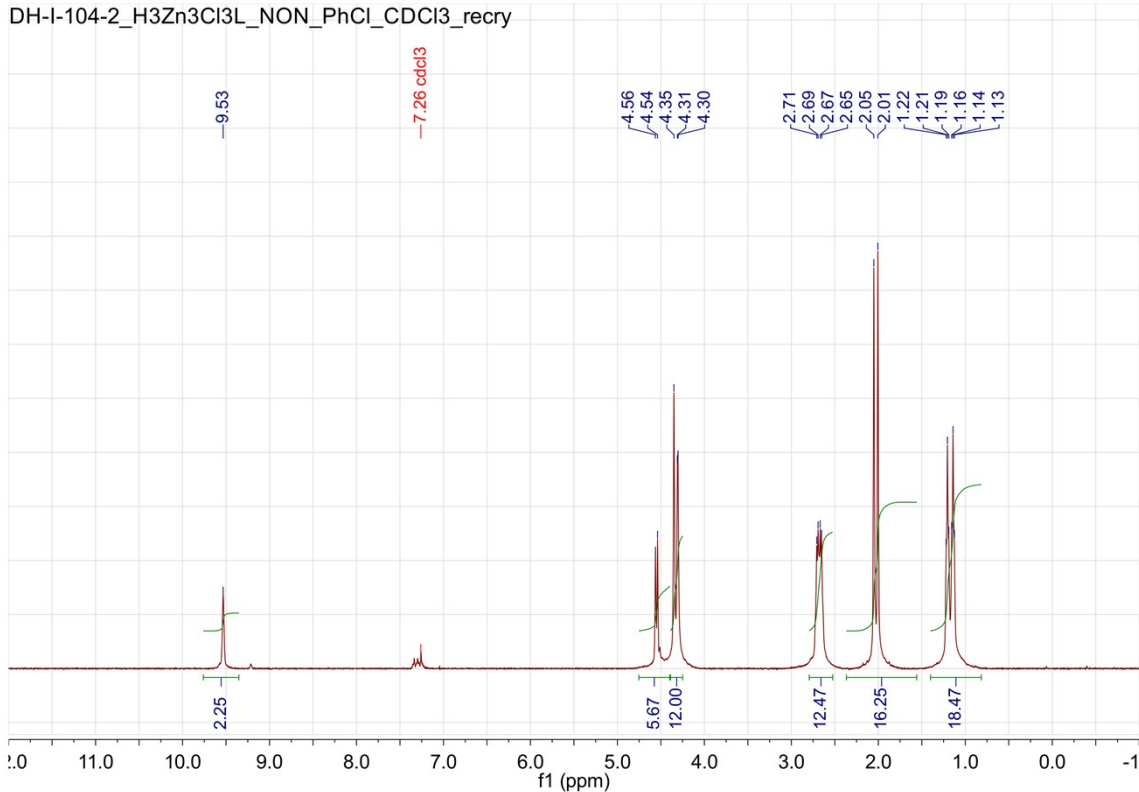
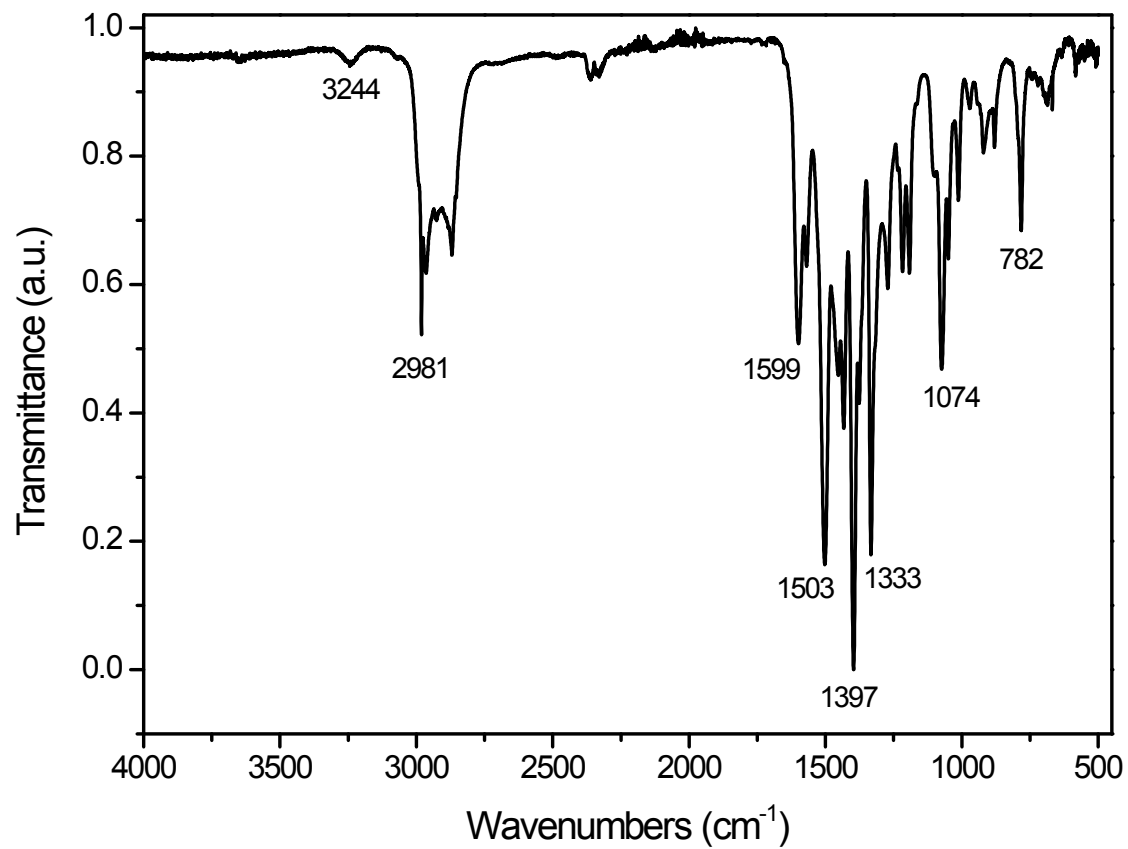


Figure S8. Infrared spectrum of **1**

DH-I-104-2\_H3Zn3Cl3L\_NON\_PhCl\_CDCl<sub>3</sub>\_recry



**Figure S9.** <sup>1</sup>H NMR spectrum (CDCl<sub>3</sub>, 500 MHz) of **2**



**Figure S10.** Infrared spectrum of **2**

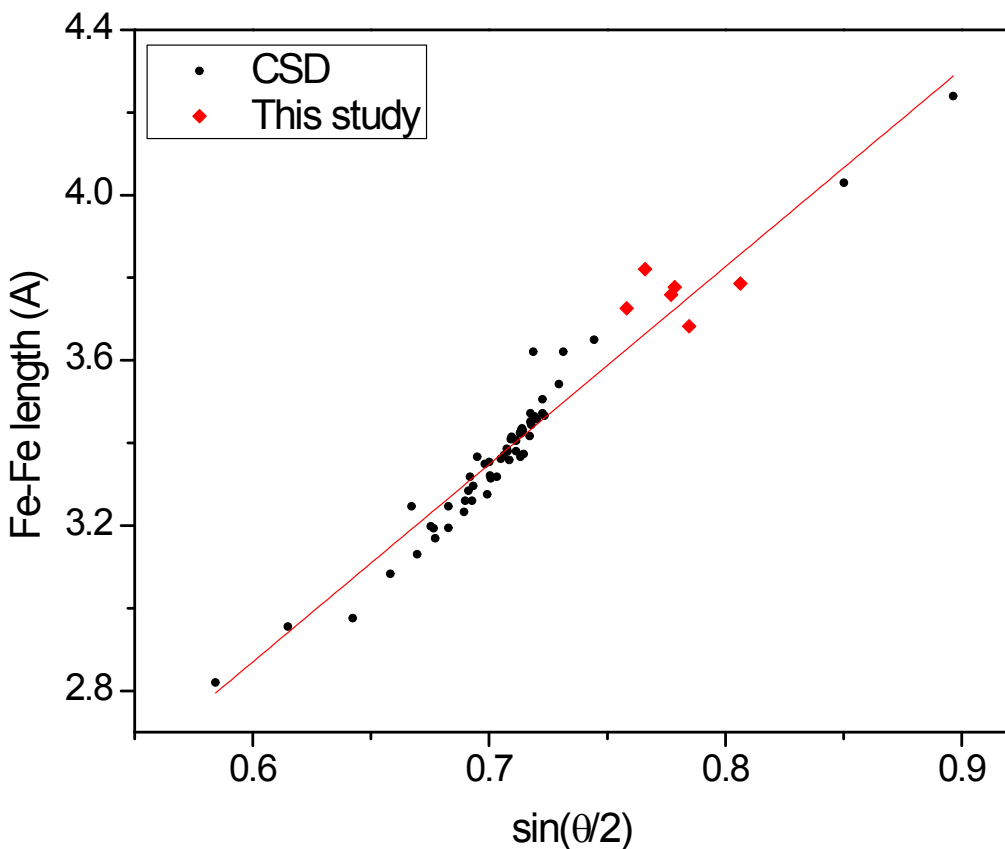


**Figure S11.** Fe–Fe bond length plotted versus  $\sin(\theta/2)$ , where  $\theta$  is the angle of Fe–Cl–Fe. The straight line calculated from  $d_{Fe-Fe} = 4.783 \sin^{[rot]}(\theta/2)$  Å with  $R^2=0.99976$ . The slope represents twice the bond length of Fe–( $\mu$ -Cl).

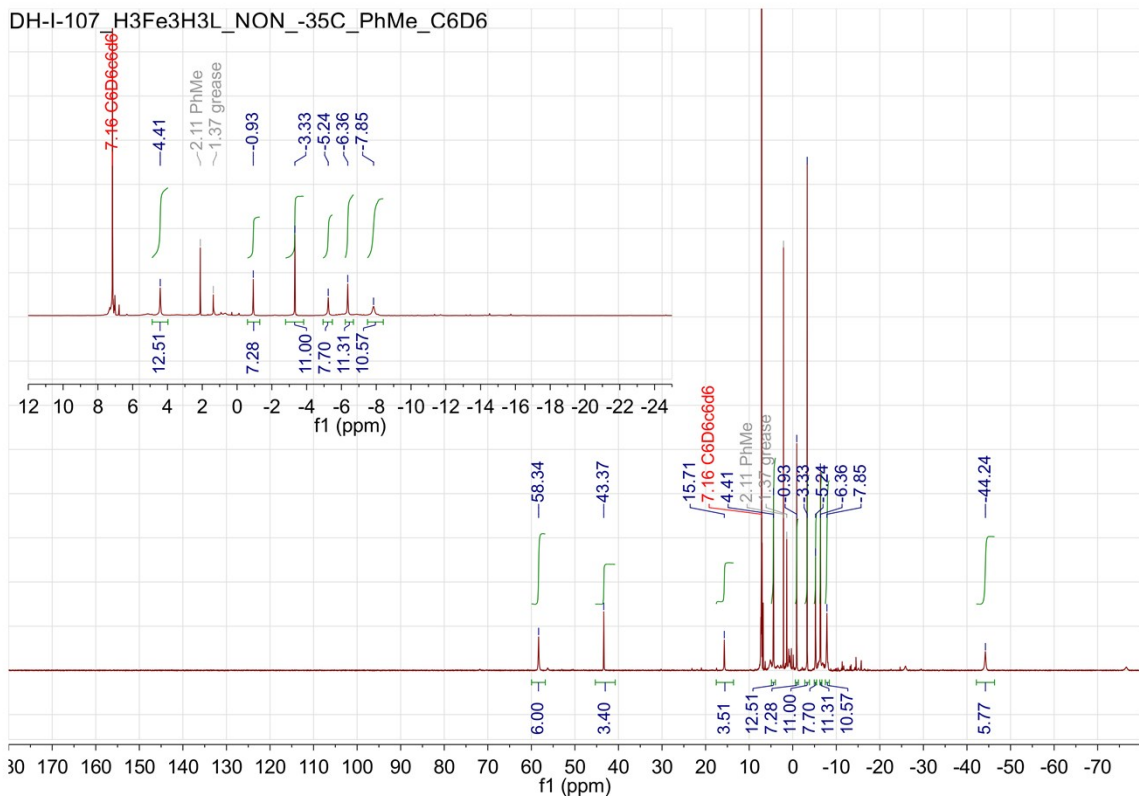


**Figure S12.** Paramagnetic  $^1\text{H}$  NMR spectrum ( $\text{C}_6\text{D}_6$ , 500 MHz) of **3**

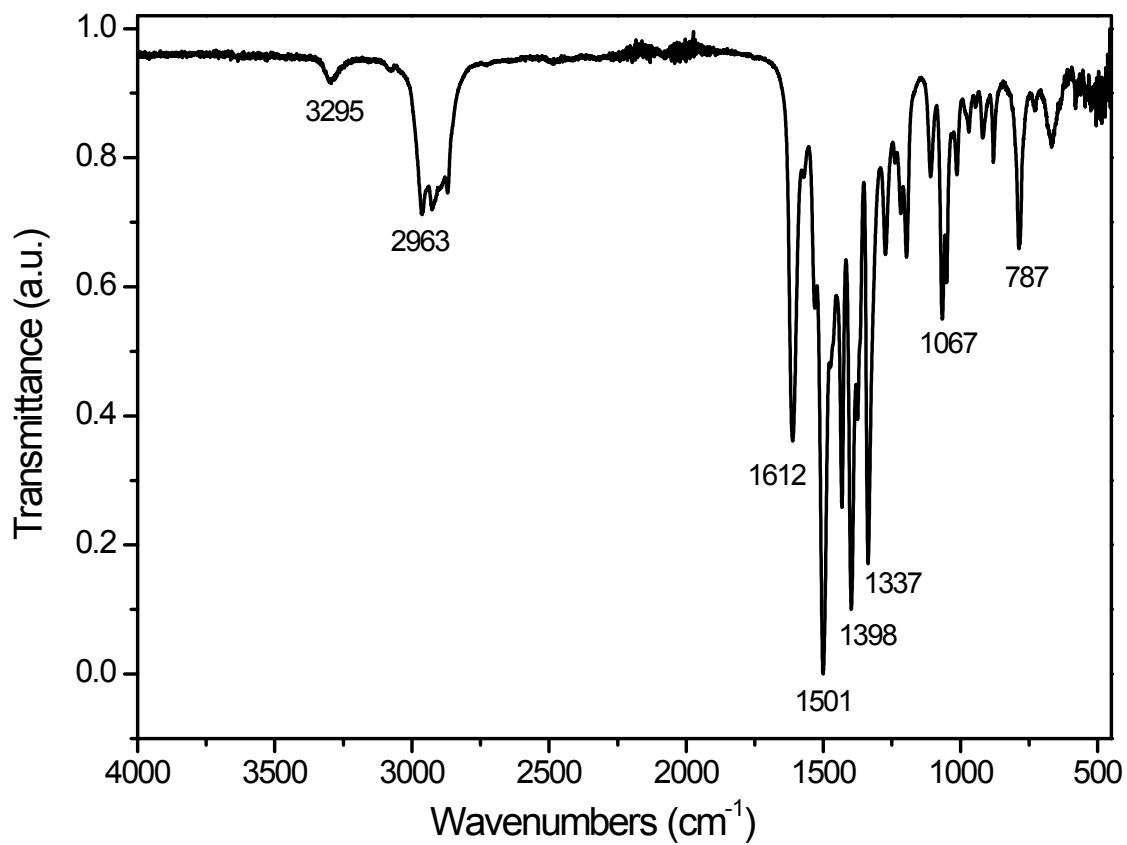


**Figure S13.** Infrared spectrum of **3**

DH-II-69-1\_H3Zn3H3L\_NON\_C6D6\_recryst

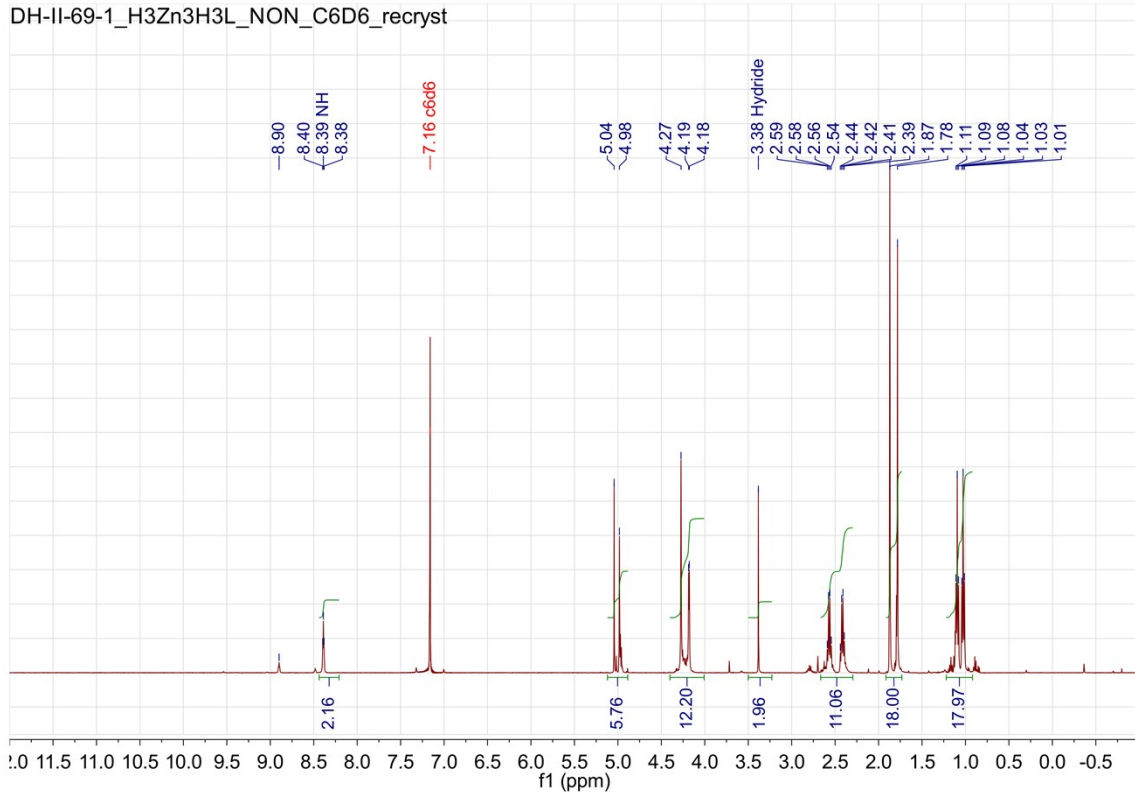


**Figure S14.** <sup>1</sup>H NMR spectrum ( $C_6D_6$ , 500 MHz) of 4

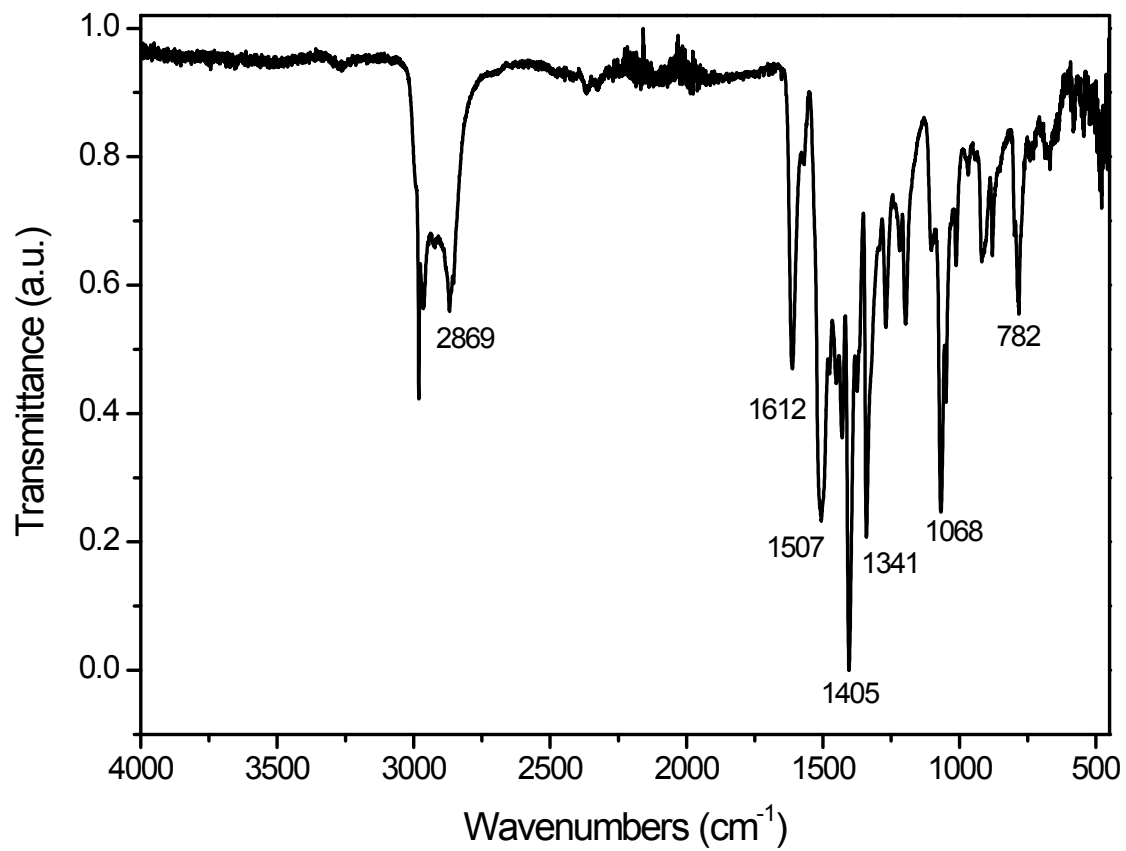


**Figure S15.** Infrared spectrum of 4

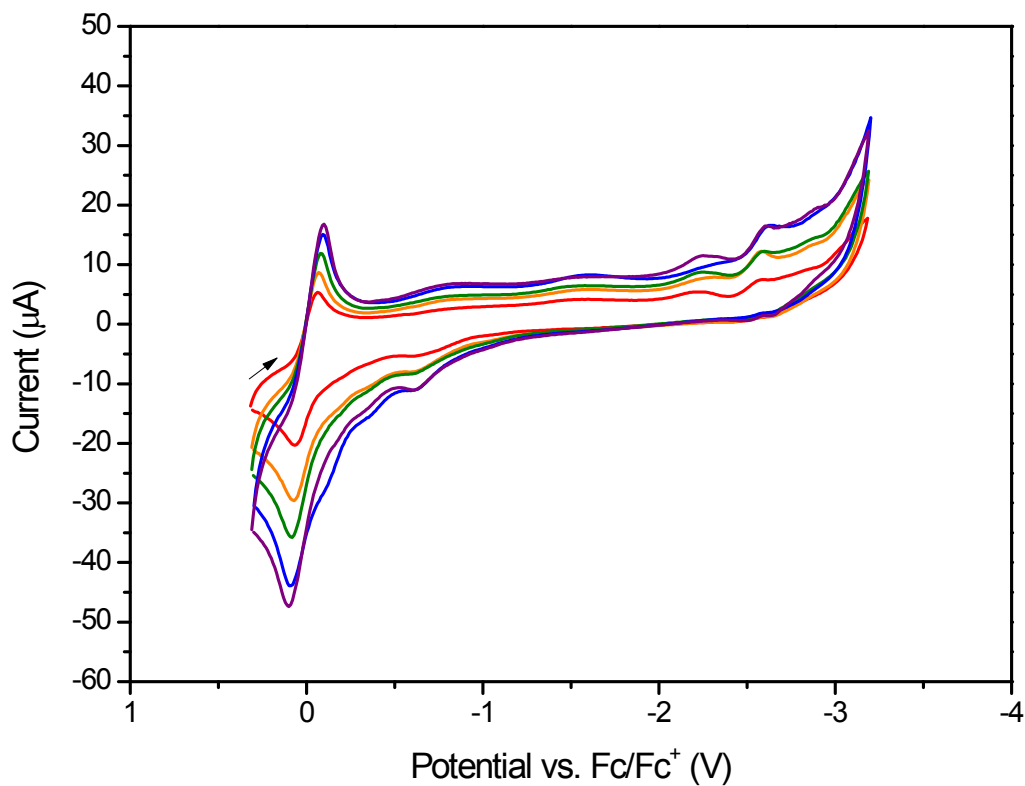


**Figure S16.** Cyclic voltammograms of **1** (0.87 mM) in THF using 0.30 M  $[\text{Bu}_4\text{N}] \text{PF}_6$  as a supporting electrolyte. Ferrocene (1.1mM) was used as internal standard. Electrodes printed on a chip was used. Working electrode: Pt; reference electrode: Ag/AgCl; counter electrode: Pt; scan rate: 100–500 mV/s.

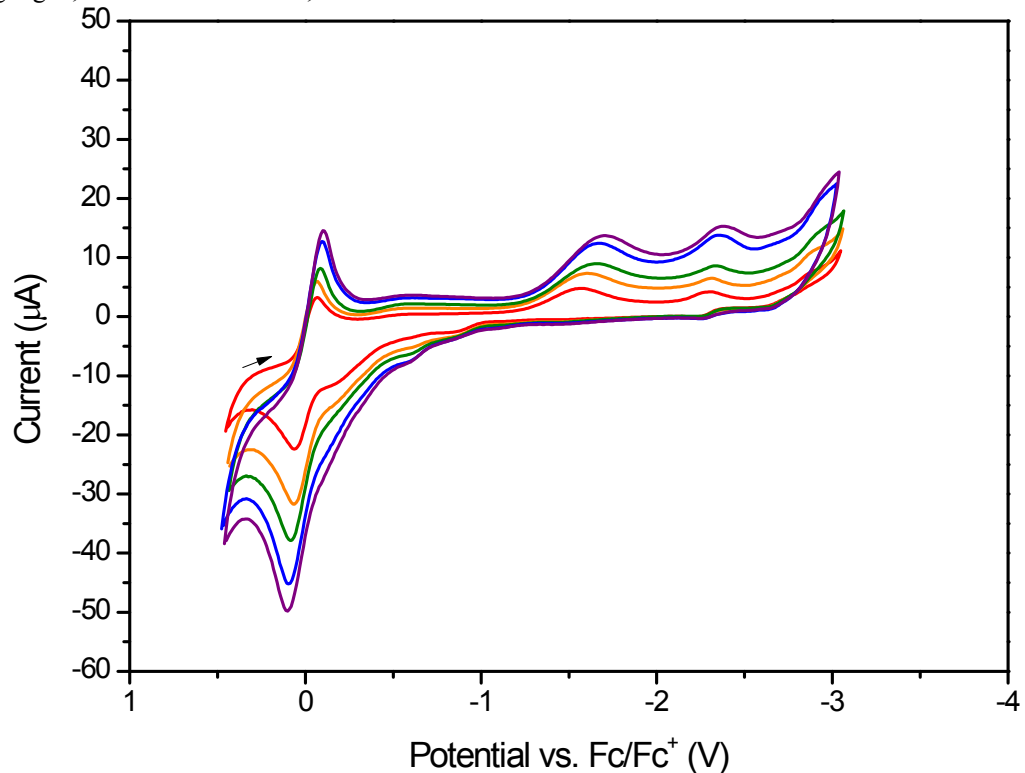


**Figure S17.** Cyclic voltammograms of **3** (0.87 mM) in THF using 0.30 M  $[\text{Bu}_4\text{N}] \text{PF}_6$  as a supporting electrolyte. Ferrocene (1.1mM) was used as internal standard. Electrodes printed on a chip was used. Working electrode: Pt; reference electrode: Ag/AgCl; counter electrode: Pt; scan rate: 100–500 mV/s.

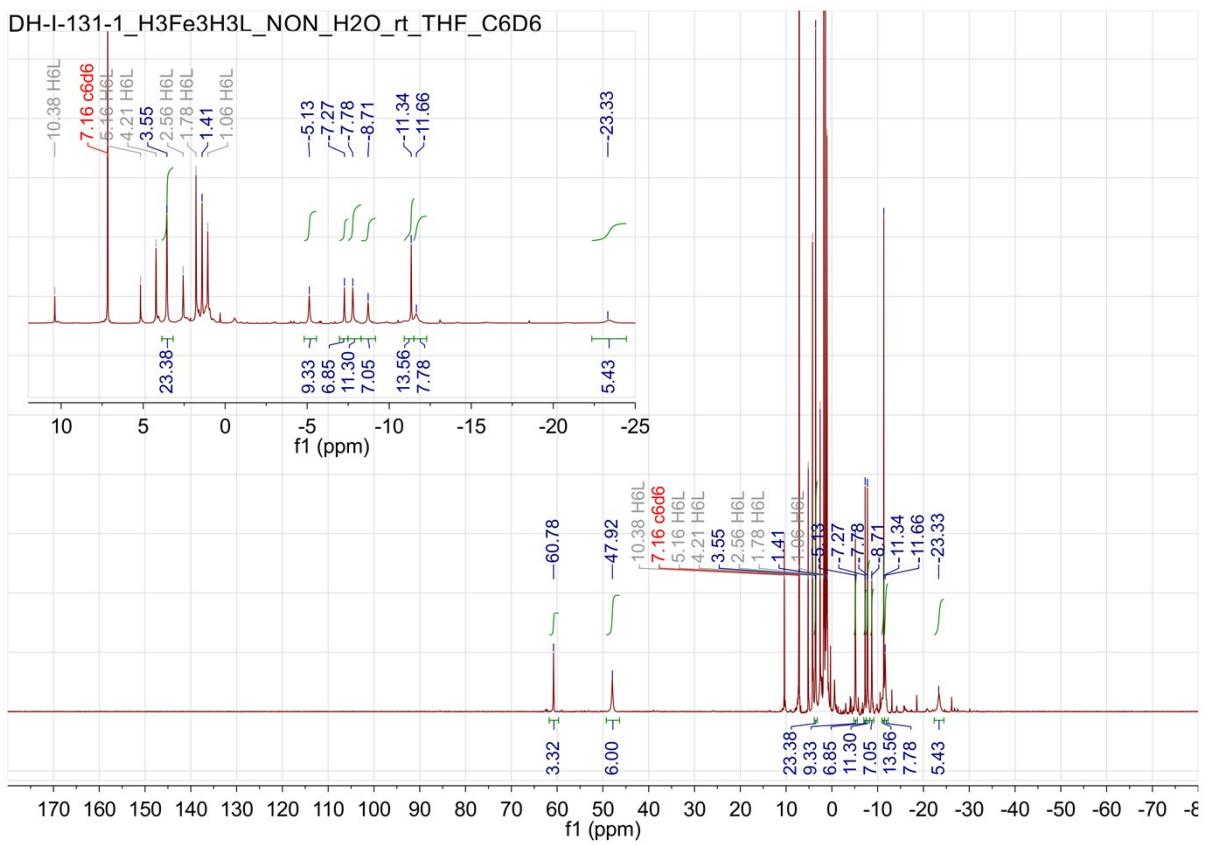


Figure S18.  $^1\text{H}$  NMR spectrum ( $\text{C}_6\text{D}_6$ , 500 MHz) of **3+H<sub>2</sub>O**

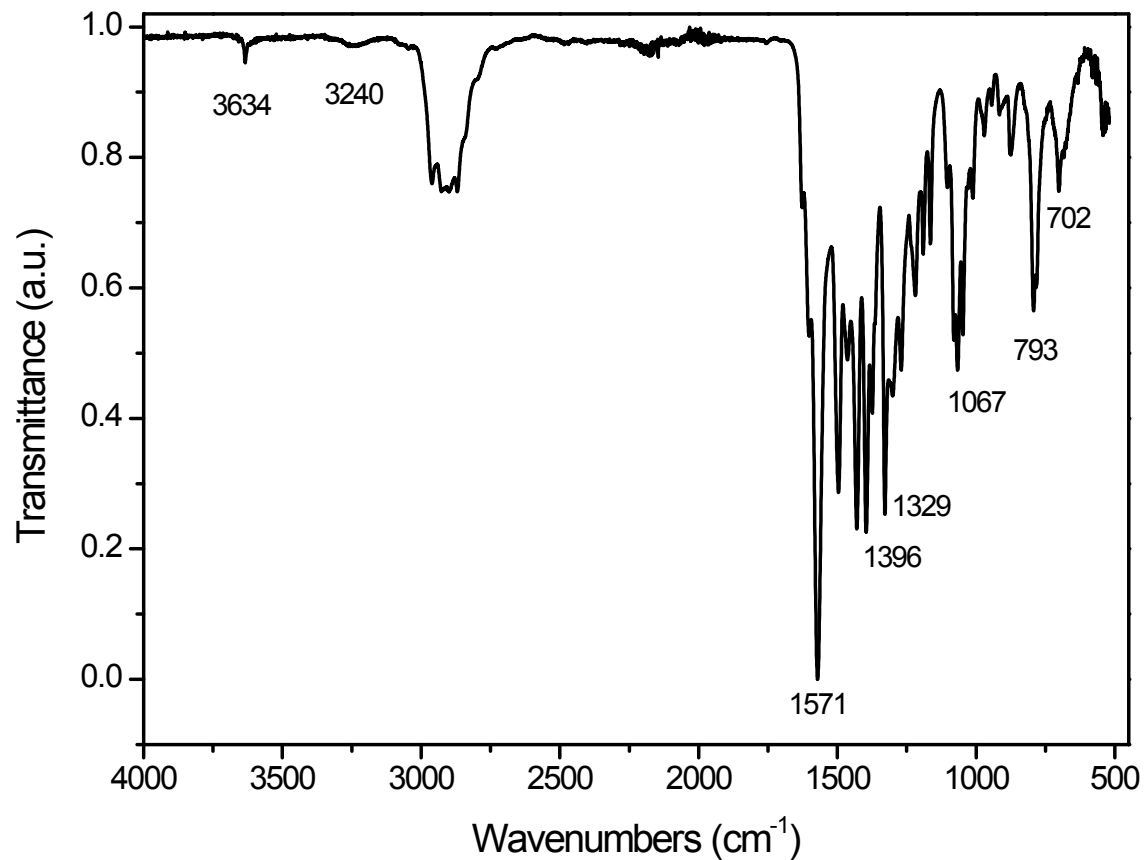


Figure S19. Infrared spectrum of **3+H<sub>2</sub>O**

**Table 1.** Crystal data and structure refinement for **1**.

Empirical formula	C72 H90 Cl3 Fe3 N6 O3		
Formula weight	1361.39		
Temperature	100(2) K		
Wavelength	0.71073 Å		
Crystal system	Monoclinic		
Space group	P2 <sub>1</sub> /n		
Unit cell dimensions	a = 12.9148(13) Å	α = 90°.	
	b = 22.857(2) Å	β = 98.891(2)°.	
	c = 23.150(2) Å	γ = 90°.	
Volume	6751.9(12) Å <sup>3</sup>		
Z	4		
Density (calculated)	1.339 Mg/m <sup>3</sup>		
Absorption coefficient	0.806 mm <sup>-1</sup>		
F(000)	2868		
Crystal size	0.469 x 0.036 x 0.024 mm <sup>3</sup>		
Theta range for data collection	1.259 to 24.999°.		
Index ranges	-15≤h≤15, -27≤k≤27, -27≤l≤27		
Reflections collected	66004		
Independent reflections	11889 [R(int) = 0.1954]		
Completeness to theta = 24.999°	100.0 %		
Absorption correction	None		
Refinement method	Full-matrix least-squares on F <sup>2</sup>		
Data / restraints / parameters	11889 / 0 / 827		
Goodness-of-fit on F <sup>2</sup>	1.012		
Final R indices [I>2sigma(I)]	R1 = 0.0829, wR2 = 0.1434		
R indices (all data)	R1 = 0.1764, wR2 = 0.1646		
Extinction coefficient	n/a		
Largest diff. peak and hole	0.469 and -0.580 e.Å <sup>-3</sup>		

## 2. References

- (1) Guillet, G. L.; Sloane, F. T.; Ermert, D. M.; Calkins, M. W.; Peprah, M. K.; Knowles, E. S.; Čižmár, E.; Abboud, K. A.; Meisel, M. W.; Murray, L. J. Preorganized Assembly of Three Iron(Ii) or Manganese(Ii)  $\beta$ -Diketiminate Complexes Using a Cyclophane Ligand. *Chem. Commun.* **2013**, 49 (59), 6635 DOI: 10.1039/c3cc43395a.
- (2) Lee, Y.; Jeon, I.-R.; Abboud, K. A.; García-Serres, R.; Shearer, J.; Murray, L. J. A  $[3\text{Fe}-3\text{S}]^{3+}$  Cluster with Exclusively  $\mu$ -Sulfide Donors. *Chem. Commun.* **2016**, 52 (6), 1174–1177 DOI: 10.1039/C5CC07813J.